Remote Sens. **2015**, *7*, 12265-12281; doi:10.3390/rs70912265

OPEN ACCESS

remote sensing

ISSN 2072-4292

www.mdpi.com/journal/remotesensing

Article

Characteristics of Surface Deformation Detected by X-band SAR Interferometry over Sichuan-Tibet Grid Connection Project Area, China

Yunshan Meng [1,2], Hengxing Lan [1,*], Langping Li [1], Yuming Wu [1,2] and Quanwen Li [1,2]

[1] State Key Laboratory of Resources and Environmental Information System, Institute of Geographic Sciences and National Resources Research, Chinese Academy of Sciences, 11 A Datun Road, Chaoyang District, Beijing 100101, China; E-Mails: mengys@lreis.ac.cn (Y.M.); lilp@lreis.ac.cn (L.L.); wymc817@163.com (Y.W.); liqw@lreis.ac.cn (Q.L.)

[2] University of Chinese Academy of Sciences, Beijing 100049, China

* Author to whom correspondence should be addressed; E-Mail: lanhx@lreis.ac.cn; Tel.: +86-10-6488-8783; Fax: +86-10-6488-9630.

Academic Editors: Salvatore Stramondo and Prasad S. Thenkabail

Received: 16 June 2015 / Accepted: 14 September 2015 / Published: 21 September 2015

Abstract: The Sichuan-Tibet grid connection project is a national key project implemented in accordance with the developmental needs of Tibet and the living requirements of 700 thousand local residents. It is the first grid project with special high voltage that passes through eastern margin of the Tibetan Plateau. The ground deformation due to widely distributed landslides and debris flow in this area is the major concern to the safety of the project. The multi-temporal interferometry technique is applied to retrieve the surface deformation information using high resolution X-band SAR imagery. The time series of surface deformation is obtained through the sequential high spatial and temporal resolution TerraSAR images (20 scenes of X-band TerraSAR SLC images acquired from 5 January 2014 to 12 December 2014). The results have been correlated with the permafrost activities and intensive precipitation. They show that the study area is prone to slow to moderate ground motion with the range of −30 to +30 mm/year. Seasonal movement is observed due to the freeze-thaw cycle effect and intensive precipitation weather condition. Typical region analysis suggests that the deformation rate tends to increase dramatically during the late spring and late autumn while slightly during the winter time. The correlations of surface deformations with these two main trigger factors were further discussed. The deformation curves of persistent scatterers in the study area showing the distinct seasonal characteristics

coincide well with the effect of freeze-thaw cycle and intensive precipitation. The movement occurring at late spring is dominated by the freeze-thaw cycle which is a common phenomenon in such a high-elevated area as the Tibetan Plateau. Intensive precipitation plays more important role in triggering landsides in the summer season. The combining effect of both factors results in fast slope movement in May. The results also suggest that the movement often occur at the middle to toe part of the slope where the combining effect of freeze-thaw cycle and precipitation plays an important role. Therefore the majority of transmission towers are not threatened significantly by geological hazards since they are located on the higher elevation which is beyond the boundary of slope movement. The comparison between field observations and the persistent scatterers interferometry (PSI) results reveals good agreement in obvious deformation accumulations. High uncertainty still exists due to issue of SAR imagery quality and the persistent scatterers interferometry technique. Nevertheless, this study provides an insight into understanding the characteristics of ground movement trend in the complicated eastern Tibet area.

Keywords: Sichuan-Tibet grid; surface deformation; PSI; freeze-thaw cycle effect; landslide

1. Introduction

The Tibetan Plateau (TP), recognized as the third pole of Earth, is the world's highest plateau, with an average altitude of over 4000 m. The terrible weather, high altitude, steep terrain, lack of transport facilities and sparely distributed settlements result in the high cost of the construction of power transmission system and the restrictive coverage of power grid in the Tibetan Plateau. The Sichuan-Tibet grid connection project is the first special high voltage grid project constructed in the Tibetan Plateau, which aims to solve the electricity shortage problem in parts of eastern Tibet and western Sichuan province. The project consists of two grid lines. The 500 kv grid line connecting Xiangcheng County, Sichuan and Changdu City, Tibet is about 500 km long. The 220 kv grid line connecting Basu County, Tibet, and Jiangda County, Tibet is about 250 km long. The two grid lines intersect at Changdu City, Tibet (Figure 1).

The grid connection project area is located in the eastern margin of Tibetan Plateau. The infrastructure projects in this area are not only threatened by active earthquakes and other tectonic movements, but also threatened by the hostile natural environment in Tibet [1]. The freeze-thaw cycle activities, heavy and intensive precipitation during rainy season, as well as a large temperature difference between day and night have grievous effects on the stability of the land surface. The high altitude and harsh weather conditions make the Tibetan Plateau the largest permafrost area in the low-middle latitudinal zone of the world. Different from the permafrost area with high latitude, e.g., Canada and Russia, the stability of permafrost in the Tibetan Plateau is relatively poor mainly because of the strong sunlight in the plateau [2]. Moreover, the temperature of the Tibetan Plateau tends to increase under the influence of global warming, which is a disadvantage to the permafrost stability [3]. Hence, continuing high temperature in the Tibetan Plateau that leads to the melting of snow and freeze-thaw effect is one of the most important factors that induce geological hazards. For example, Yigong landslide

which is a large hazard happened in Nyingchi area Tibet in April 2000 for the thawing effect of frozen soil [4]. Therefore, the freeze-thaw problem has become a major concern for hazard prevention and construction in permafrost areas.

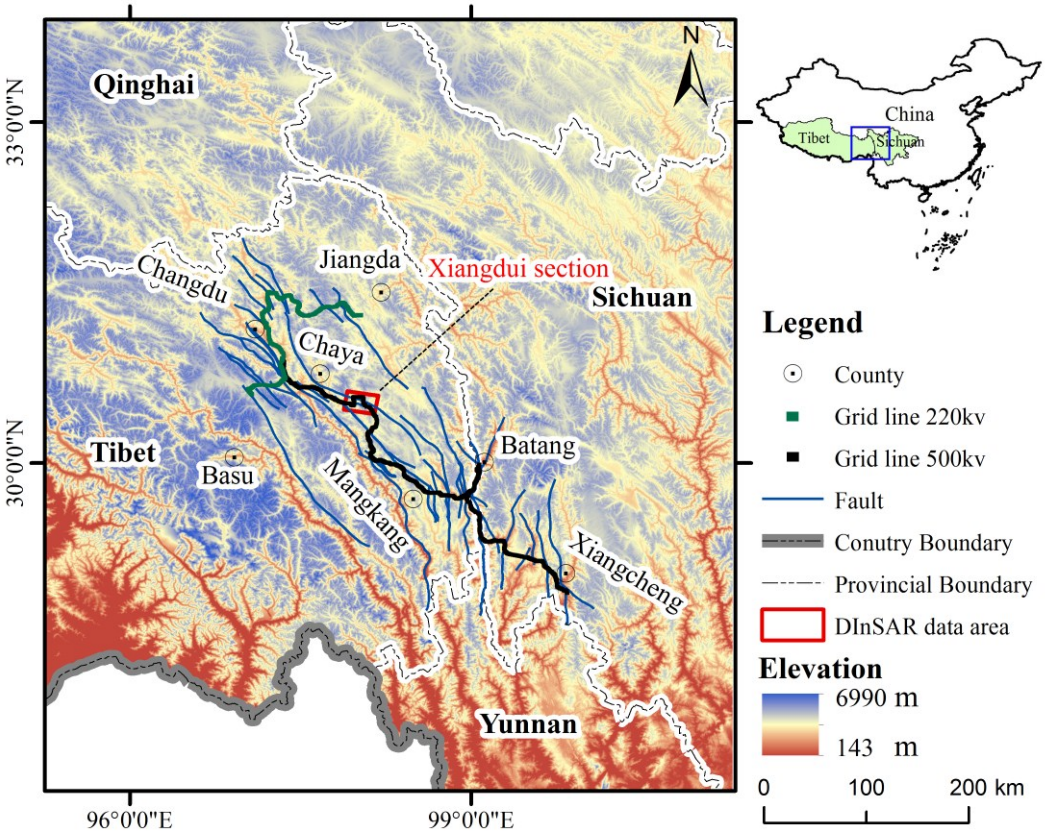

Figure 1. Overview of the grid project area with elevation displayed as background. Grid lines with different colors represent different voltage levels. Major tectonic faults adjacent to the grid lines are also shown. The red frame indicates the SAR study area.

Another important factor that caused surface deformation in southeast Tibet is heavy and intensive precipitation. Affected by terrain, precipitation in the Tibetan Plateau is mainly concentrated in south and southeast Tibet. According to the meteorological data, heavy and intensive precipitation mainly occurs in the summer and accounts for about 80 percent of the annual precipitation. The intensive precipitation could induce different levels of floods, and it is also the major triggering factor of geological hazards. The surface deformation caused by freeze-thaw cycle effect and its impact on the construction and maintenance of infrastructure in the Tibetan Plateau have already been revealed by many researches [5,6]. However, there is still a lack of studies on the twofold effect of freeze-thaw cycle effect and precipitation on to the surface deformation in high-elevated regions such as the Tibetan plateau. Therefore, based on the special weather condition in southeastern Tibet, it is essential to study the surface deformation results from the combined influences of freeze-thaw cycle effect and precipitation over a one year period.

The project area passes through the rigorous and remote Tibetan Plateau, it is thus difficult and costly to apply point-based surface deformation monitoring techniques such as GPS and leveling. The space-borne differential synthetic aperture radar interferometry (DInSAR) is capable of mapping surface deformation over extensive area with high resolution and high precision [7,8]. However, the results

obtained from DInSAR analysis have sometimes suffered from temporal and geometrical de-correlations, and have been strongly affected by atmospheric inhomogeneities, especially in vegetated or low reflectivity homogeneous regions. In order to overcome these problems, many technologies have been presented, and Persistent Scatterers Interferometry (PSI) technique is one of the most prominent [9]. With the availability of large stacks of SAR images acquired over the same areas, long time series of deformation can be analyzed using PSI techniques [10,11]. PSI techniques have been widely and successfully used for the assessment of geological hazards, such as landslides [10,12,13], land subsidence [14], and earthquakes [15].

This paper is organized as follows. The background of the grid connection project and the study area are introduced firstly, followed by a description of the datasets and the methodology based on PSI technique. Then, the results are presented, and the possible reasons that caused the observed deformations are discussed. The purpose of this research is to provide a baseline for detecting potential large scale geological hazards and further mitigating their hazard effects in the project area.

2. Study Area

A section around the Xiangdui town, Chaya County, Tibet was selected as the experimental site (Figures 1 and 2), primarily for its accessibility as well as the availability of field observation data. Maiqu River and Changqu River are two major rivers in this study area. Most of the tributaries of the major rivers running along the valleys are seasonal rivers. There are several villages sparsely distributed in flat areas along the river or in some lower valleys. The largest settlement, Xiangdui town, is located in the northwest of the study area where the two major rivers meet. The main roads in the study area run along the major rivers. The grid line in this study area is about 50 km in length and has 77 transmission towers. In order to avoid the influence of potential geological hazards, transmission towers are generally not constructed in lower valleys.

The topography is mainly an alpine canyon with a prominent relief. The average altitude of the study area is about 4100 m, and the relative height difference varies between 200 and 500 m. The action of geomorphic agents such as temperature variations, stream and freeze-thaw activity are relatively strong. The bedrock geology of the study area is dominated by Cretaceous and Jurassic strata. The study area comprises rock masses mainly composed of sandstones, mudstones, conglomerate, and limestone. Due to the influences of the tectonic activities and weathering in the surface, the joint network of rocks there is complex and the loose materials are widely distributed. Those loose materials rested on high and steep slopes are favorable for the formation of geological hazards.

A detailed geological hazard investigation about Tibet was conducted by the Institute of Geological Environment and Hazard Prevention of Tibet in 2005. The geological hazards that greatly threaten the main roads, factories, villages and towns were recorded. The type and scale of the geological hazards as well as the factors that induced the hazards were recorded. According to this investigation, there were 18 geological hazards distributed in the study area, including six debris flows and twelve landslides. Prior to the construction of the electricity transmission project, geomechanical, geomorphological, and geological hazards surveys were also conducted by manual inventory in the project area.

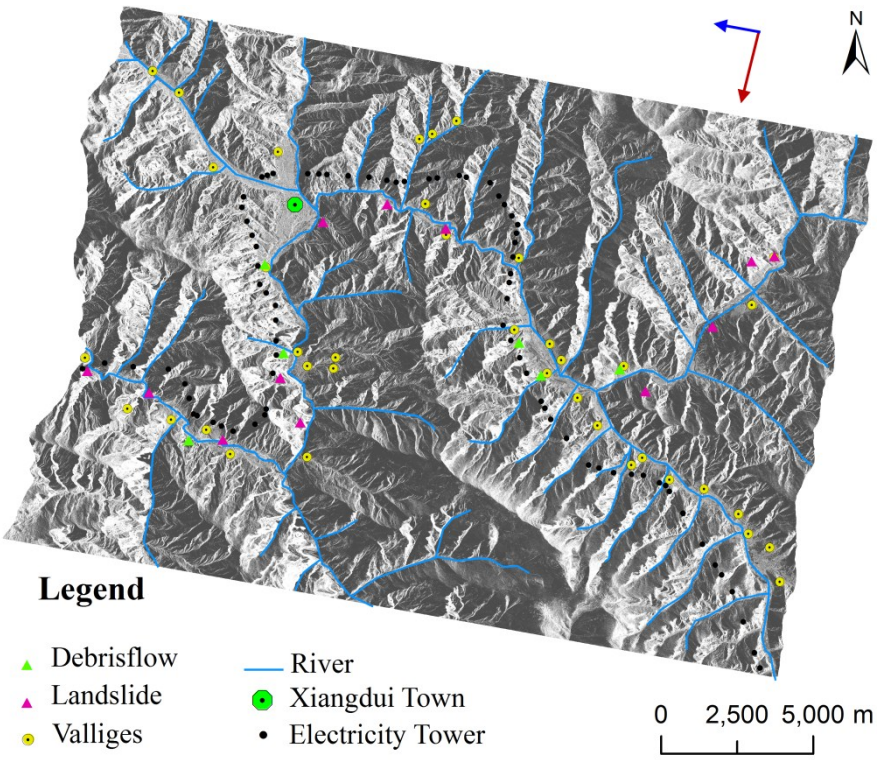

Figure 2. The locations of transmission towers, geological hazards, residential sites, and major rivers in the study area are shown on the SAR intensity map.

The climate type of the study area is defined as montane warm temperate zone with arid valleys climatic. The annual average temperature in the study area is about 9 °C. According to the temperature data from Chaya county meteorological station, the temperature rises above freezing point in the early April, and falls below freezing point in October (Figure 3). The average annual precipitation is about 1400 millimeters. The rainy season lasts from May to September and accounts for about 70% of the annual total precipitation (Figure 3). The daily precipitation data is a type of raster data with 0.5 degree space resolution released by China Meteorological Administration. Monthly records show that precipitation in the study area has a double peak: one in May and another in July.

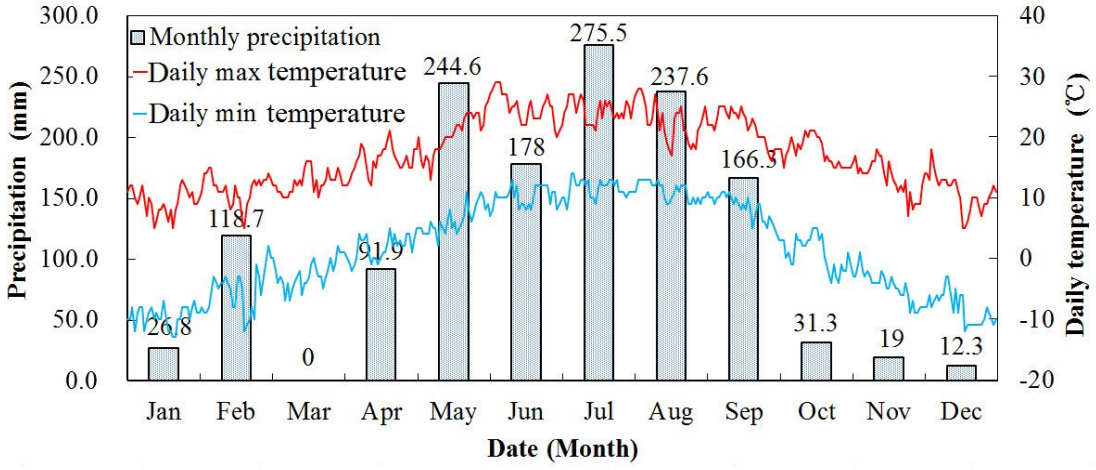

Figure 3. Meteorological data of the study area in 2014.

3. Datasets and Procedure of SAR Image Processing

3.1. Datasets

The long term surface deformation monitoring in the study area are taken for almost a year. As listed in Table 1, 20 TerraSAR-X images acquired from 5 January 2014 to 12 December 2014 were analyzed in this study. The SAR images present pixel spacing of 1.3 and 1.9 m in range and azimuth, respectively. The datasets were acquired in descending orbit with similar incidence angles of about 41°. The data coverage area is shown in Figure 2 and with a red frame in Figure 1. The three arc-second (~ 90 m) shuttle radar topography mission (SRTM) DEM data from the United States Geological Survey (USGS) were used for topographic phase estimation at the first step, and then for geocoding the X-band InSAR data, *i.e.*, transforming range-Doppler coordinates into Universal Transverse Mercator map geometry system. In addition, optical images obtained by unmanned aerial vehicle (UAV)-borne and space-borne sensors were used to assist the interpretation of surface deformations derived from PSI analysis.

Table 1. TerraSAR-X images used in this study.

Pairs[a]	Acquisition Time (dd-mm-yyyy)	Perpendicular Baseline (meters)	Temporal Baseline (days)
1	05-01-2014	−349.947	−198
2	23-03-2014	−183.955	−121
3	06-05-2014	−216.038	−77
4	17-05-2014	−97.387	−66
5	28-05-2014	46.561	−55
6	08-06-2014	−178.422	−44
7	19-06-2014	−257.969	−33
8	30-06-2014	−95.031	−22
9	11-07-2014	−101.388	−11
10	22-07-2014	0	0
11	02-08-2014	−108.411	11
12	13-08-2014	−82.749	22
13	24-08-2014	−35.041	33
14	04-09-2014	−160.889	44
15	15-09-2014	−7.731	55
16	26-09-2014	−169.581	66
17	07-10-2014	−295.993	77
18	18-10-2014	−257.564	88
19	09-11-2014	−123.437	110
20	12-12-2014	−64.736	143

[a] The image acquired on 22 July 2014 was selected as the reference for SLC image co-registration to minimize the distances of available SAR acquisitions in the temporal domain.

3.2. Procedure of SAR Image Processing

The Interferometric Point Target Analysis (IPTA) technique, one of the PSI techniques [16,17], was used in processing the time series of high resolution TerraSAR-X images. The IPTA processing on the time series of low resolution SAR images [18,19], or high resolution TerraSAR-X SAR images [20,21] had been successfully used to investigate earth surface deformations in a mm/year scale.

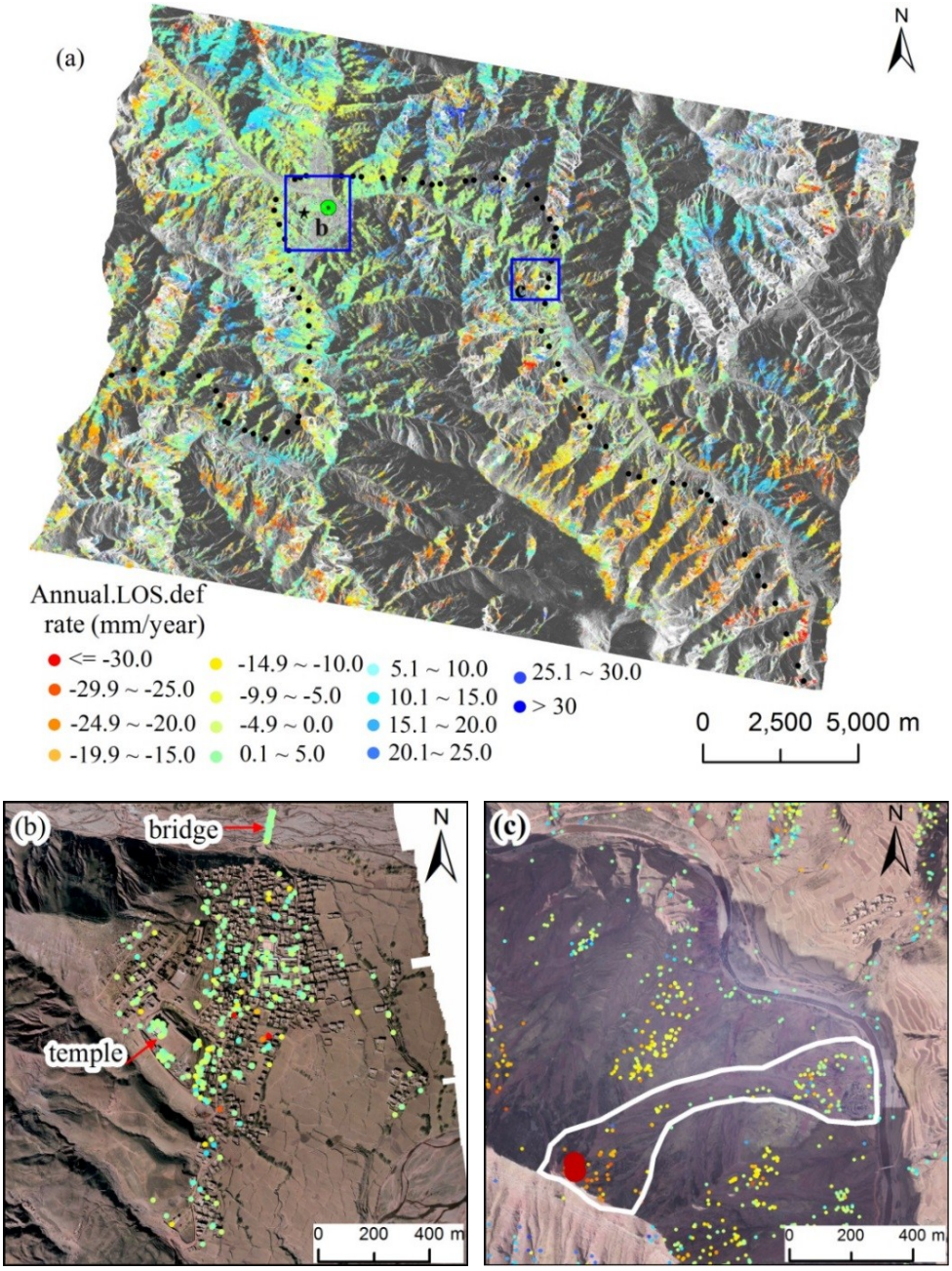

Figure 4. The PSI monitoring results of the whole study area. (**a**) The reference point is located on the top of a temple (shown as a black start in the upper figure). (**b**) The rectangular frames show the locations of the Xiangdui township and (**c**) a small scale landslide.

In IPTA approach, the image recorded on 22 July 2014 was chosen as the common master SAR image, and others are slave images. A multi-looking with two-by-two in range and azimuth direction was used to derive InSAR products with approximately four-meter ground resolution. 20 differential interferograms (including master-master image pair) were generated after the removal of the topographic and flat earth phase components. The minimum cost flow (MCF) method [22] was used for phase unwrapping. The Xiangdui township shows high coherence in most of the interferograms. This is a benefit to choosing the reference point. A point located on a building in a stable sub-region in the Xiangdui township, which shows a high coherence value of 0.95, was chosen as the reference point (marked by the star in Figure 4). Point targets, such as bare rocks and man-made facilities (e.g., bridges

and buildings), do not show the speckle behavior associated with distributed targets since a single coherent scatterers dominated the echo. Low spectral diversity criterion of detecting persistent scatterers (PSs) takes those well-focused point targets whose backscattering intensities almost keep constant when processing different looks with fractional azimuth and range bandwidths as PS candidates. It is worth mentioning that, due to the polarizations of SAR images being VV, the outlines of buildings in the SAR image are relatively blurry. As towers were constructed during the monitoring period, the deformation history of transmission towers cannot be gotten with PSI techniques. After quality control, the density of PS points is about 421 per square kilometers. The high spatial density of PS points is owing to two aspects: (1) TerraSAR-X image has high spatial resolution, allowing identification of small features on earth surface; (2) the vegetation coverage in the study area is poor, thus sufficient bare rocks could be identified as PS candidates.

The IPTA processing was carried out using the GAMMA interferometric software. The IPTA results consist of the improved heights, linear deformation rates, atmosphere phase delays, refined baselines, quality information, and linear and non-linear deformation history for each PS point. It must be emphasized that, the PSI results only measured the relative displacements compared with a local reference point.

4. Results

4.1. Spatial Pattern of Surface Deformation

Active deforming areas are revealed by a map of average line of sight (LOS) deformation velocities (Figure 4). Positive LOS velocities represent movements towards the satellite, while negative LOS velocities represent movements away from the satellite. The PSI monitoring results of the Xiangdui township and a small landslide adjacent to the Changqu River are also shown in Figure 4.

Accordingly to Figure 4a, local positive displacement can be found in some areas, with a maximum velocity of more than +20 mm/year. The deformation movements towards the satellite occur mainly at the foot of landslides. The activity of landslides under gravity usually results in loose deposits accumulated at the feet of steep slopes. Therefore, a slight positive could be observed at the foot of landslides. Further investigation revealed that negative displacement in the study area is most significant on the steep slopes of landslides. In addition, the deformation rates in the points away from satellite are correlated with the positions in landslides. Generally, the deformation rate exhibits a tendency of reducing with the drop of position from top to toe of landslides (Figure 4c).

The results did not reveal significant deformations around the Xiangdui township. The LOS deformation rate varies between −10 and +10 mm/year (Figure 4b). Similarly, the sparsely distributed villages in the study area (Figure 2) are also not threatened by severe land deformations or geological hazards. In other words, the majority of residential sites in the study area, especially the Xiangdui township, were relatively stable during the one year observation period. The monitoring results coincide with common senses, since the locations of settlements in mountainous areas are the result of mutual adaptations between human beings and natural hazards, for example subsidence, landslides, debris flows, and earthquakes, *etc.*

4.2. The Characteristics of Surface Deformation

Based on the SAR monitoring results, the surface deformation in temporal dimension was analyzed. In addition, the correlations between observed surface deformation and freeze-thaw cycle effect as well as intensive precipitation were discussed. The deformation history of one site was selected as an example to show the effects of freeze-thaw cycle processes and precipitation on surface deformation. The positions of the points are shown in Figure 4c (marked by a red point).

During the one year monitoring period, there are two periods where freeze is the dominant factor that lead to surface deformation (Figure 5). The first period is from January to early April. Since average min temperature has been below zero, the surface of the monitoring sites is relatively stable without the influence of heavy precipitation and artificial disturbance. The second period is from October to December. When average min temperature falls below zero in October, frozen soil gradually forms. As the soil water changes from liquid to solid during the freeze process, the deformation rates of unstable slopes are relatively reduced. With the deepening of frost heave and the volume of soil water expands, the landslide tends toward a stable state. For example, the deformation rates of the point (a) and point (b) are relatively low during the period from October to December compared with the period from April to September (Figure 5). According to the meteorological record, average min temperature rises above zero in April. When temperature eventually rises again, the frozen soil melts. The thaw effect of frozen soil becomes the main reason for the surface deformation. During the thaw process, the sufficient soil water and its decreased volume make the sedimentation rate of unstable surface dramatically increased. For example, the deformation rate of all point (a) and point (b) in Figure 5 show an increasing negative displacement trend during the period from early April to May, especially in early May with the additional impact of intensive precipitation. Similar to the deformation situation of the Yigong landslide that happened in April, this phenomenon can be ascribed to the rapid deformation caused by the thawing effect of frozen soil, melting snow, and intensive precipitation [4].

Based on field investigation, debris flow is one of the most serious geological hazards in the study area. Most debris flows originally occur in the form of precipitation-induced landslides before they move into a valley channel. Precipitation, especially in the form of rainstorms, is one of the main factors that induce landslides in the study area during the rainy season.

The rainy season of the study area usually starts in May and lasts until September. According to meteorological data, intensive precipitations were mainly concentrated from July to September last year. The rain records during the observation time can be categorized into two classes according to the criterion of China Meteorological Administration: light rain (<10 mm/day) and moderate rain (10–25 mm/day). There are more than 200 rainy days all over the monitoring year in the study area, including 79 light rainy days and 31 moderate rainy days. All through the rainy season from May to September, precipitation hardly stopped. Relative intensive precipitation periods include: (1) 1st to 8th May; (2) 26th to 31st May; (3) 12th to 31st July; (4) 7th August to 4th September; and (5) 16th to 28th September. The results of TerraSAR-X time series of LOS displacement rate allowed us to explore the relationship between precipitation and slide movements. The deformation history of a specific site was presented to show the relationship between intensive precipitation and surface deformation (Figure 5).

As shown in Figure 5, with the increase of precipitation in May, the deformation rate of the landslide also rises. On the contrary, as the amounts and the times of precipitation go down in October (Figure 3),

the deformation rate also correspondingly decreases. The landslide motion is almost consistent with intensive precipitation.

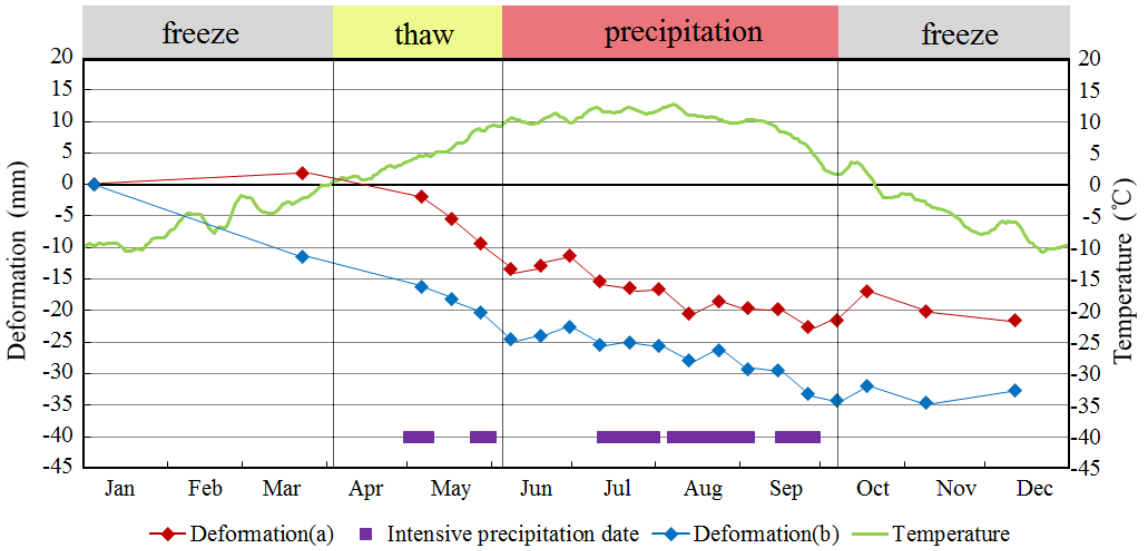

Figure 5. TerraSAR-X PSI monitoring results for landslides with different terrains. The deformation histories of the persistent scatterers sited on landslide and the average seven-days min temperature as well as intensive precipitation time periods are also shown. The locations of landslides are shown in the Figure 4.

5. Discussions

5.1. Freeze-Thaw Cycle Effect and Water Content

Seasonally and perennially frozen soils occupy the whole project area. Depending on factors such as slope aspect, altitude, geological structure, rock characteristics and underground water content, the thickness of frozen soil generally varies between 1.2 and 2.5 m. The freeze-thaw cycle activities continually happen as temperature periodically changes over a year. Seasonal freeze-thaw of soil water is accompanied by a series of physical processes, such as water transfer and heat exchange [23]. When seasonal frozen soil melts in summer, the soil water gradually changes from solid to liquid, and the subsidence of ground surface accelerates. On the contrary, the soil water changes from liquid to solid during the freezing process. As the temperature decreases, the alleviation of land subsidence is obvious, and a slight uplift even happens in some areas. The cyclic freeze-thaw processes of frozen soil would destroy geological environment, and further result in geological hazards, such as landslides and rock falls [24]. Therefore, the freeze-thaw cycle effect of frozen soil in the study area can do great harm to human projects.

Seasonal frozen soil is a special soil water system where ice and water coexist, and the higher the amount of ice, the poorer the soil stability is. Hence, the deformation history of a specific site with different water content was analyzed to show the effects of freeze-thaw processes on surface deformation (Figure 6). From Figure 6, it is suggested that the deformation histories of persistent scatterers in this site have distinct seasonal characteristic and coincides well with the cycle of freeze-thaw. The main sessions of freeze heave process in the monitoring period include from January to

April and from October to December. The deformation rates of unstable slopes are relatively reduced more because the volume of soil water expands as it becomes solid in October. Moreover, due to lower positions are close to rivers with sufficient water supply, the surface deformation rate gradually increases as elevation decreases from the top to foot of slopes (Figure 6 marked as green frame).

As the average min temperature rises above zero in early April, the frozen soil begins to melt. Then, the sufficient soil water and its decreased volume cause the sedimentation rate of unstable surfaces to dramatically increase. For example, the deformation rate of all points in Figure 6b show an increasing subsidence trend during the period from early April to May. Soils near rivers contain more water, and thus can become completely frozen in cold seasons. Hence, subsidence rate exhibits a tendency of increasing with the drop of position from top to toe of unstable slope (Figure 6 marked as red frame).

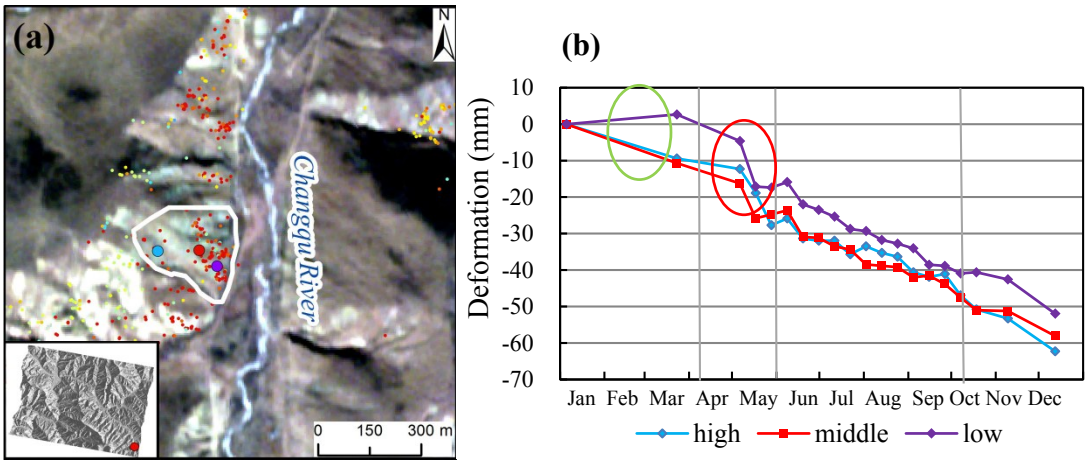

Figure 6. TerraSAR-X PSI monitoring results for an unstable surface on the banks of Changqu River. (**a**) The location of this unstable surface is shown in the insert figure. (**b**) The time series deformation histories of three points with different elevations are also shown.

In general, the water table directly affects soil frost heave. Most of the places along the project area belong to weak freeze-thaw zone. However, some places with sufficient surface water and groundwater, for example places adjacent to rivers, are regarded as strong freeze-thaw zone and thus are severely affected by freeze-thaw activity [25]. In order to protect the transmission towers from the freeze-thaw effects, the transmission towers are constructed in elevated lands with low groundwater level. Furthermore, waterproof procedures and drainage systems were adopted to ensure the safety and quality of constructions.

Intensive precipitation and freeze-thaw activities were very important factors controlling the surface deformation in the study area (Figures 5 and 6b). Precipitation can not only increase self-weight and gliding thrust of slopes, but also can lubricate the sliding surface of the slope when surface water penetrates into underground and further lead to the increase of seepage force and pore pressure. In addition, intensive precipitation and large day-night temperature differences can easily cause rock cracking, through which surface water would infiltrate into rocks. Increased flow in the near surface groundwater system and the saturation of soil may increase pore pressure and decrease the effective strength of the failure surface, and eventually trigger movement. This indicates that precipitation may play a role in the initiation and acceleration of sliding (from May to September). It is worth noting that,

the freeze activity induced by the declining temperature might be another factor to the alleviating deformation trend since October.

5.2. The Safety of Sichuan-Tibet Electricity Transmission Project

The safety of transmission towers distributed in the study area is analyzed in this section. Only 55 of the 77 transmission towers could be monitored with the method of PSI techniques. This is because only SAR images acquired in descending orbit were used. The uneven terrain leads some transmission towers hidden in the radar shadows.

Nevertheless, the results show that the majority of towers are safe since they are located within higher elevated safety areas which are beyond the boundary of slope movement. Only a few towers such as tower 74A are found to be threatened by significant surface deformation. This tower lies on a steep slope. The slope gradient varies between 50 and 55 degrees. The bedrock around the tower had been heavily weathered. The adverse geological conditions and steep topography result in the issue of slope stability. The monitoring results coincide with the field survey results. A quick deformation, with a maximum velocity of more than −20 mm/year, happens on the top of the mountain (Figure 7a). In addition, there are two small active areas with subsidence phenomenon near the tower (Figure 7a), which had raised concerns with agencies in charge.

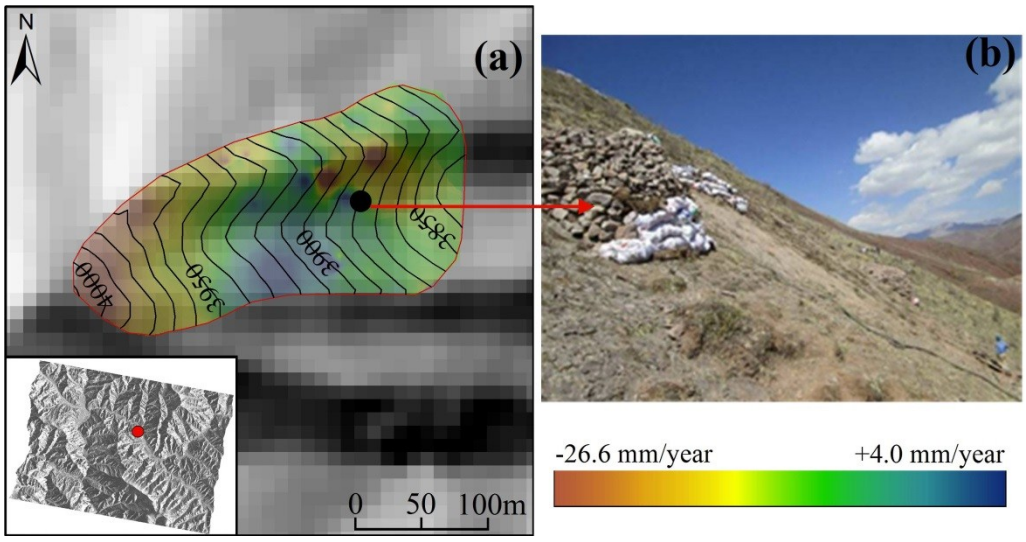

Figure 7. The PSI results around transmission tower 74A are shown using Inverse Distance Weighting interpolation. (**a**) The tower shown with a black point lies on one side of a ridge. (**b**) The photo shows the deposits located near one leg of the tower. The location of this tower is shown in the insert figure.

Results also suggest that the towers located in the southeast part of study area might suffer from the slope instability. Field investigation found high density of gullies distributed in the southeast region of the study area. In rainy season, the gullies will become ditches, through which water runs into the Changqu River with loose materials. The slopes of this area are composed of argillaceous rocks formed in stratified structure. The surface of rock has been heavily weathered, and the depth of weathering could reach to 2.5 m. A thin layer of residual soil covers the land surface. This loose earth becomes the main source of materials of debris flows, which could threaten the safety of the project in the future.

The monitoring results show that, compared with other regions of the study area (e.g., Figure 8a,b), distinct subsidence distributed in the southeast region (Figure 8c). Most of permafrost in Tibet belongs to a warm permafrost category which is sensitive to the change of temperature and moisture [26,27]. The water content in the southeast region is relatively high owing to high density of tributaries of rivers. Therefore, the southeast region is more vulnerable to the freeze-thaw cycle effect, especially under the artificial construction conditions.

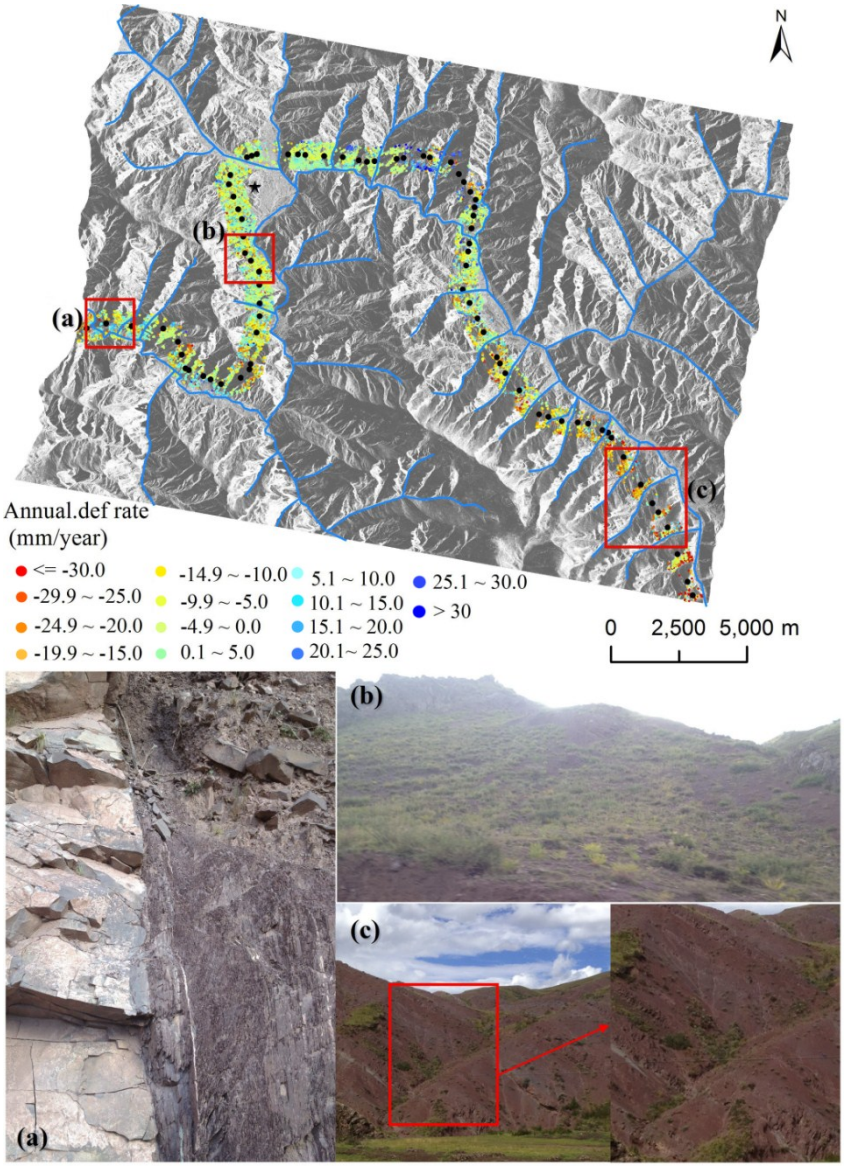

Figure 8. The surface deformation field along the grid line is shown. Photos (**a**), (**b**) and (**c**) show the landscapes of different areas.

5.3. Uncertainty of the Results

The issue of uncertainty comes from the data quality, data process, and result interpretation. The data quality is the first concern for this study. The TerraSAR data used in this research have a higher ground resolution of 3 m. Such data are able to reveal more ground details, but also results in more point-like targets, not object-like targets. Compared with ENVisat ASAR (C-band, 5.6 cm) and ALOS PALSAR (L-band, 23.6 cm), TerreSAR (X-band, 3.2 cm) dataset working with a shorter wavelength has a poor

ability to penetrate the vegetation, and thus results in low coherence interferograms in vegetated permafrost areas. The small density of persistent scatterers will probably induce unwrapping errors in some areas resulting incorrect deformation information. Moreover, the dataset available for this study is only descending. It is therefore difficult to differentiate between real vertical and horizontal motion of the ground. Both ascending and descending orbit data should be acquired in the future study in order to extract both horizontal and vertical components of the slope movement. In addition, the temperature data used are not totally within the region covered by SAR images which might results in the uncertainty of the correlation analysis between the deformation and the triggering factors.

There is still an issue for the data processing using PSI technique. The high quality of refinement of the data processing might be difficult due to the high topographical effect in the Tibetan plateau and the drawback of SAR dataset. More robust coherent targets and more robust topographical and atmospheric effect removal will highly improve enhance the precision of the deformation result.

In addition, the data interpretation may also result in uncertainties, especially the error analysis. According to statistics, the mean value and standard deviation of uncertainties of deformation rate are 2.34 mm/year and 0.78, respectively. Hence, whether the displacements can be regarded as errors should be taken into consideration in the areas where the deformation values are less than 3 mm.

Nevertheless, combining with the field observations, the study results reveals the characteristics of the overall deformation trends which establish a good foundation for the further detailed analysis.

6. Conclusions

The Sichuan-Tibet Grid connection project passes through southeastern of the Tibetan Plateau with adverse natural environment and wide spread geological hazards. Ground stability is the key issue for the safety of the project. An integrated analysis is conducted using high spatial and temporal resolution X-band SAR with precipitation and temperature data. Intensive precipitation and freeze-thaw activities were found to be the two most important factors controlling the surface deformation in the study area. The understanding of the characteristics of ground movement is important for the construction and maintenance of Grid infrastructures in the Tibetan Plateau. In this study, taking Xiangdui section, Changdu area of Tibet, as the experimental site, we examined the characteristics of surface deformation results from the combined influence of freeze-thaw cycle effect and intensive precipitation.

The main conclusions of this study can be summarized as follows:

(1) The results reveal surface deformation characteristics in the study area. The study area is prone to slow to moderate ground motion with the range of −30 to +30 mm/year. The slow point targets with deformation towards the satellite are found to be distributed on the toe of landslides. This is consistent with the observation that the foot of landslide will slightly uplift when loose deposits accumulated at the feet of steep slopes. On the other hand, with varied temperature and wide distributed frozen soil, frozen heave often causes obvious deformation of surface ground in the area with sufficient water content. As expected, the point targets with slow movements away from satellite are mostly distributed on active slopes. Temporal variations of surface deformation reveal non-linear deformation histories.

(2) Intensive precipitation and freeze-thaw cycle activities were found to be the two most important factors controlling the surface deformation characteristics and the seasonal movement trend in the

study area. During the one year monitoring period, surface deformation that was caused by freeze heave was mostly from October to early April of next year. Then, as the rise of temperature since early April, thaw of the frozen soil was the dominant factor that lead to surface subsidence before rainy season came. During the rainy season, mainly from May to September, intensive precipitation was the most important cause of surface deformation. Moreover, the heave and subsidence movement of the frozen soil with sufficient water content was more remarkable compared with other areas. Such regions are primarily located from the middle to toe of the slope where large movements often occur.

(3) The results suggest that the majority of the monitored transmission towers are located in stable areas. However a few towers which are located in the steep highly weathered slopes and southeast part of study area are still suffering from the issue of the slope instability. These vulnerable towers to be threatened by surface deformation were successfully detected by the significant surface subsidence in PSI results.

Results uncertainties still exist mainly due to data quality, processing, and the interpretation. For example, the inherent feature of TerraSAR imagery generates more point-like scattering targets, less robust coherent object-like targets in such high-elevated study area. In addition, it is difficult to obtain real ground motion using single orbit SAR dataset. Nevertheless, this study provides an insight into understanding the characteristics of ground movement trend in the complicated eastern Tibet area. It provides the foundation for the future detailed long-term SAR Interferometry monitoring on the ground movement in the Tibet region.

Acknowledgments

This work was financially supported by the Natural Science Foundation Project of China under Grant No. 41272354 and Grant No.41472282. The authors would like to express their appreciation to the China power engineering consulting group corporation Beijing North Star Co. Ltd for their TerraSAR-X data support. The authors would also like to thank China Meteorological Administration for their meteorological data support.

Author Contributions

All of the authors conceived of and designed the study. Yunshan Meng analyzed the data and wrote the paper. Hengxing Lan is the corresponding author and he is mainly responsible for data discussion and wrote part of this paper. Langping Li improved the English writing. Yuming Wu and Quanwen Li contributed on the data collection.

Conflicts of Interest

The authors declare no conflict of interest.

References

1. Wang, L.; Wu, Z.; Sun, J.; Liu, X.; Wang, Z. Characteristics of ground motion at permafrost sites along the Qinghai-Tibet Railway. *Soil Dyn. Earthq. Eng*. **2009**, *29*, 974–981.

2. Wang, P. *Using D-InSAR to Monitor the Motion of Frozen Ground in Qinghai-Tibet Plateau*; Central South University: Changsha, China, 2009.
3. Wu, Q.B.; Hou, Y.D.; Yun, H.B.; Liu, Y.Z. Changes in active-layer thickness and near-surface permafrost between 2002 and 2012 in alpine ecosystems, Qinghai-Xizang (Tibet). *Glob. Planet Chang*. **2015**, *124*, 149–155.
4. Xu, Q.; Shang, Y.J.; Asch, T.V.; Wang S.T.; Zhang, Z.Y.; Dong, X.J. Observations from the large, rapid Yigong rock slide-debris avalanche, southeast Tibet. *Can. Geotech. J*. **2012**, *49*, 589–606.
5. Chang, L.; Hanssen, R. Detection of permafrost sensitivity of the QingHai-Tibet railway using satellite radar interferometry. *Int. J. Remote Sens*. **2015**, *36*, 691–700.
6. Jin, L.; Wang, S.; Chen, J.; Dong, Y. Study on the height effect of highway embankments in permafrost regions. *Cold Reg. Sci. Technol.* **2012**, *83*, 122–130.
7. Massonnet, D.; Rossi, M; Carmona, C.; Adragna, F.; Peltzer, G.; Feigl, K.; Rabaute, T. The displacement field of the landers earthquake mapped by radar interferometry. *Nature* **1993**, *364*, 138–142.
8. Rosi, A.; Agostini, A.; Tofani, V.; Casagli, N. A procedure to map subsidence at the regional scale using the persistent scatterer interferometry (PSI) technique. *Remote Sens*. **2014**, *6*, 10510–10522.
9. Xie, C.; Li, Z.; Xu, J.; Li, X. Analysis of deformation over permafrost regions of Qinghai-Tibet plateau based on permanent scatterers. *Int. J. Remote Sens*. **2010**, *31*, 1995–2008.
10. Ferretti, A.; Prati, C.; Rocca, F. Nonlinear subsidence rate estimation using permanent scatterers in differential SAR interferometry. *IEEE T. Geosci. Remote.* **2000**, *38*, 2202–2212.
11. Ferretti, A.; Prati, C.; Rocca, F. Permanent scatterers in SAR interferometry. *IEEE T. Geosci. Remote*. **2001**, *39*, 8–20.
12. Colesanti, C; Ferretti, A; Novali, F.; Prati, C; Rocca, F. SAR monitoring of progressive and seasonal ground deformation using the permanent scatterers technique, *IEEE T. Geosci. Remote*. **2003**, *41*, 1685–1701.
13. Canuti, P.; Casagli, N.; Ermini, L.; Fanti, R.; Farina, P. Landslide activity as a geoindicator in Italy: Significance and new perspectives from remote sensing. *Environ. Geol*. **2004**, *45*, 907–919.
14. Ferretti, A; Bianchi, M.; Prati, C.; Rocca, F. Higher-order permanent scatterers analysis. *Eurasip J. Appl. Sig. P*. **2005**, *20*, 3231–3242.
15. Colesanti, C.; Ferretti, A.; Prati, C.; Rocca, F. Monitoring landslides and tectonic motions with the Permanent Scatterers Technique. *Eng. Geol*. **2003**, *68*, 3–14.
16. Werner, C.; Wegmuller, U.; Strozzi, T.; Wiesmann, A. Interferometric point target analysis for deformation mapping. In Proceedings of 2003 IEEE International Symposium on Geoscience and Remote Sensing, Toulouse, France, 21–25 July 2003.
17. Gamma Remote Sensing. *GAMMA Interferometric Point Target Analysis: Users Guide 2013*; Gamma Remote Sensing: Gümligen, Switzerland, 2003.
18. Lan, H.X.; Gao, X.; Liu. H.J.; Yang, Z.H.; Li, L.P. Integration of TerraSAR-X and PALSAR PSI for detecting ground deformation. *Int. J. Remote Sens*. **2013**, *34*, 5393–5408.
19. Cigna, F.; Bateson, L.; Jordan, C.; Dashwood, C. Simulating SAR geometric distortions and predicting Persistent Scatterer densities for ERS-1/2 and ENVISAT C-band SAR and InSAR applications: Nationwide feasibility assessment to monitor the landmass of great Britain with SAR imagery. *Remote Sens. Environ.* **2014**, *152*, 441–466.

20. Lan, H.X.; Li, L.P.; Liu, H.J.; Yang, Z.H. Complex urban infrastructure deformation monitoring using high resolution PSI. *IEEE J. Sel. Top. Appl*. **2012**, *5*, 643–651.
21. Chen, J.; Wu, J.; Zhang, L.; Zou, J.; Liu, G.; Zhang, R.; Yu, B. Deformation trend extraction based on Multi-Temporal InSAR in Shanghai. *Remote Sens.* **2013**, *5*, 1774–1786.
22. Costantini, M. A novel phase unwrapping method based on network programming. *IEEE T. Geosci. Remote*. **1998**, *36*, 813–821.
23. Chen, F.L.; Lin, H.; Li, Z.; Chen, Q.; Zhou J. Interaction between permafrost and infrastructure along the Qinghai-Tibet Railway detected *via* jointly analysis of C-band and L-band small baseline SAR interferometry. *Remote Sens. Environ*. **2012**, *123*, 532–540.
24. Chen, F.L.; Lin, H.; Zhou, W.; Hong, T.H.; Wang, G. Surface deformation detected by ALOS PALSAR small baseline SAR interferometry over permafrost environment of Beiluhe section, Tibet Plateau, China. *Remote Sens. Environ*. **2013**, *138*, 10–18.
25. Li, S.S.; Li, Z.W.; Hu, J.; Sun, Q.; Yu, X.Y. Investigation of the seasonal oscillation of the permafrost over Qing -Tibet Plateau with SBAS-InSAR algorithm. *Chin. J. Geophys*. **2013**, *56*, 1476–1486. (In Chinese)
26. Jin, H.J.; Li, S.X; Wang, S.L. Impacts of climatic change on permafrost and cold regions environments in China. *Acta Geogr. Sin*. **2000**, *55*, 161–173. (In Chinese)
27. Yuan, S.C.; Zhang, L.X.; Han, L.M.; Cao, Y.X. Influences of environmental conditions on construction safety reliability of Qinghai-Tibet Railway in permafrost region. *Chin. J. Eng. Geol*. **2006**, *14*, 433–437. (In Chinese)